Hindawi Publishing Corporation
Journal of Spectroscopy
Volume 2013, Article ID 103602, 6 pages
http://dx.doi.org/10.1155/2013/103602

Research Article

Influence of the Crystal Texture on Raman Spectroscopy of the AlN Films Prepared by Pulse Laser Deposition

Jingjing Wang,[1] Da Chen,[2] Yan Xu,[2] Qixin Liu,[2] and Luyin Zhang[2]

[1] *Common Course Department, Shandong University of Science and Technology, Jinan 250031, China*
[2] *Qingdao Key Laboratory of Terahertz Technology, Department of Applied Physics, College of Science, Shandong University of Science and Technology, Qingdao 266510, China*

Correspondence should be addressed to Da Chen; phychenda@163.com

Received 8 June 2012; Accepted 28 September 2012

Academic Editor: Zhifeng Shao

We investigate the Raman scattering of the AlN films prepared by pulse laser deposition. The Raman spectrum and the X-ray diffraction (XRD) patterns of the AlN films were compared to find out the influence of the crystal texture on the Raman scattering. The E_2 (high) and A_1 (TO) scattering modes were observed in Raman spectra. The results show that the orientation and the crystal quality of the AlN films have a great impact on these Raman scattering modes. The deterioration of (002) orientation and the appearance of other orientations in the XRD patterns lead to the weakening of the E_2 (high) mode and strengthening of the A_1 (TO) mode in the Raman spectrum. In addition, the E_2 (high) peak is broadened with the increasing of the width of the X-ray rocking curve. The broadening of the Raman peaks can be associated with degeneration in crystal quality. Furthermore, by combining the energy shift of E_2 (high) mode with the measured residual stress in the films, the Raman-stress factor of the AlN films prepared by pulse laser deposition is $-4.45\ \text{cm}^{-1}$/GPa for the E_2 (high) mode.

1. Introduction

With the tremendous progress of III-nitrides research in terms of both fundamental understanding as well as devices, applications, Aluminum nitride (AlN) attracts increasing interest due to the band gap of approximately 6 eV and some excellent properties including high thermal conductivity, good stability at high temperatures, and high acoustic velocity. These excellent properties make AlN thin films useful in many applications, such as hard coatings [1], electroacoustic devices [2], buffer layers for epitaxial growth [3], buried dielectric layers in future silicon-on-insulator devices [4] and Micro/Nano-Electro-Mechanical Systems (MEMS/NEMS) [5, 6]. Recently AlN-based deep ultraviolet light-emitting diodes (LEDs) [7, 8] have been reported, which demonstrates the practicability of AlN as an active deep ultraviolet material for future optoelectronic device applications. Many methods have been used to grow AlN film including molecular beam epitaxy (MBE) [9–11], metal-organic chemical vapor deposition (MOCVD) [12, 13], pulse laser deposition (PLD) [14–16], and reactive sputtering [17, 18]. In particular, PLD is suited to grow AlN films for many applications because it is rapid and it is capable of producing high-quality, stoichiometric films at low deposition temperature [16].

In the studies of thin films, X-ray diffraction (XRD) is a strict and widely used method to measure the crystal texture. However, a good film texture is not a guarantee for high-quality devices in many applications. For example, the residual stress in the film is also important because it may alter the energy band structure and influence the device performance, particularly in LEDs and MEMS/NEMS. On the other hand, Raman scattering is widely used to detect the phonon vibration properties in materials and has been proven to be a practical method for studying stress of III-V semiconductor. At present, some reports have focused on the Raman scatterings of the AlN films grown by MBE [9, 19] or MOCVD [12]. However, there are few reports concerning the scattering characteristics of the AlN films prepared by PLD [20].

In this work, we prepared AlN films using PLD and measured their X-ray patterns and Raman spectra. These results were compared to find out the influence of the texture on the phonon mode in the AlN films. Furthermore, we study the correlation between the shift of E_2 (high) mode and the residual stress in the films.

2. Experimental Details

The AlN films were prepared using a PLD system (LMBE-II, SKY Techno. Co., Ltd.). The target was a circular, stoichiometric AlN slab with a purity of 99.99% fabricated by hot pressing (Omat Sputtering Target Co.). Before the growth of AlN films, the chamber was evacuated until the base pressure decreases to less than 2×10^{-5} Pa. The target was placed 6 cm from the substrate. A KrF excimer laser (λ = 248 nm, PRF = 30 Hz, and τ = 14 ns) with an energy density of 1–5 J/cm^2 was used to ablate the target. The laser beam was brought into the chamber through a UV fused-silica window at a 60° angle relative to the target surface normal. During the film preparation, N_2 (99.9999% purity) was introduced into the chamber and maintained at a pressure of 1 Pa. The polished 1-inch-diameter (001) sapphire was used as the substrate. The substrates were heated to 500°C and kept at this temperature during the preparation process. The thicknesses of all films were controlled to about 1 μm.

The crystal structure and the orientation of the films were identified by XRD (BRUKER-AXS) at wavelength of 0.15418 nm (Cu Kα). The morphologies of the films were observed by field effect scanning electron microscope (SEM, FEI SIRION 200) under the operating voltage of 10 kV. The Raman measurement was performed at room temperature in the backscattering configuration at the film surface using the 488 nm line from Ar^+ laser, and a double monochromator (Spex 1404) equipped with a charge-coupled device detector was employed to analyze the scattered light. The profilometer (Veeco DekTak-6) was used to measure the radius of the substrate curvature before and after the growth of AlN films, from which we obtained the residual stress according to Stoney's equation. More than five positions were measured to reduce the error of the stress across the wafer.

3. Results and Discussion

3.1. The XRD Patterns of the AlN Films. Figure 1 shows the XRD patterns of the AlN films prepared at four levels of the laser energy density. All the samples are wurtzite hexagonal structure. The films prepared at 1.3 J/cm^2 (sample A) and 2.4 J/cm^2(sample B) have two diffraction peaks around 33° and 36°, corresponding to the AlN (100) and (002) orientation, respectively. The (002) peaks become stronger and sharper with increasing the laser energy density, while the (100) peaks become weaker. This means that the (002) texture of the AlN films is improved. Moreover, sample C, which is prepared at the energy density of 3.5 J/cm^2, exhibits a single and sharp (002) diffraction peak with the full width at half maximum (FWHM) of 0.21°, indicating a preferred c-axis orientation. By Scherrer's formula, the calculated average gain

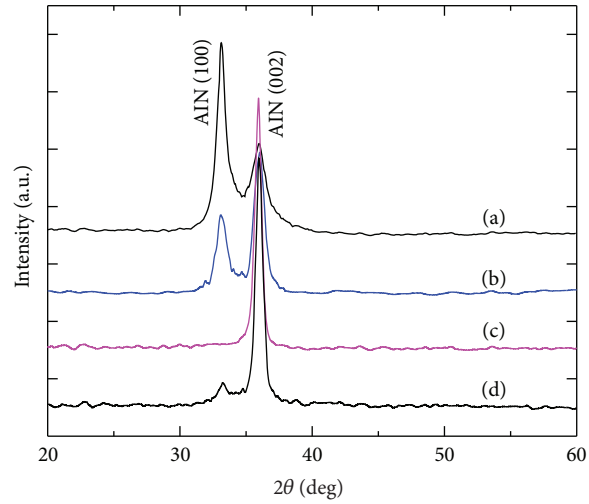

Figure 1: The XRD patterns for AlN films prepared at laser energy density of (a) 1.3 J/cm^2, (b) 2.4 J/cm^2, (c) 3.5 J/cm^2, and (d) 4.8 J/cm^2.

size of sample C is about 42 nm. As shown in Figure 2, the highly parallel columnar crystals are observed from the cross-sectional morphology. The film prepared at 4.8 J/cm^2 (sample D) has also a (002) orientation, but the FWHM of the (002) peak is about 0.35°, which is a little larger than that of sample C.

In order to describe the crystal texture of the samples in detail, the (002) plane X-ray rocking curves of the AlN films were measured as shown in Figure 3. The FWHM value of sample C (0.75°) is observed much smaller than that of sample D for AlN (002) plane, which accords with the results of XRD. The influence of the laser energy density on the film textures can be explained through the Al-N complex kinetic energy in the laser plasma. Generally, the increasing of the laser power not only enhances the sputtering yield, but also raises the kinetic energy of the particles in the laser plasma. As a result, during the higher energy plasma, the Al-N complex particles have sufficient kinetic energy to attach themselves to the substrate, hence providing the atoms with more opportunities to move to the lowest energy state and to form a highly (002) oriented crystal structure. On the other hand, the substrate may be strongly attacked if the particle kinetic energy is too large (exceeds 3.5 J/cm^2 in this experiment), resulting in the surface damage and deterioration in the (002) texture as shown in sample D.

3.2. The Raman Spectra of the AlN Films. The Raman spectrum of the samples was measured to find out the correlation between the crystal texture and the Raman scattering mode. According to the group theory, wurtzite AlN structure belongs to the space group $C_{6v}{}^4$ ($C6_3mc$) with two formula units per primitive cell. Theory analysis [19] predicts the zone-center optical modes in the representation as $= A_1 + 2B_1 + E_1 + 2E_2$. The A_1, E_1, and two E_2 modes are Raman active, while the B_1 mode is inactive. The A_1 and E_1 modes are each splited into the longitudinal optical (LO) and transverse

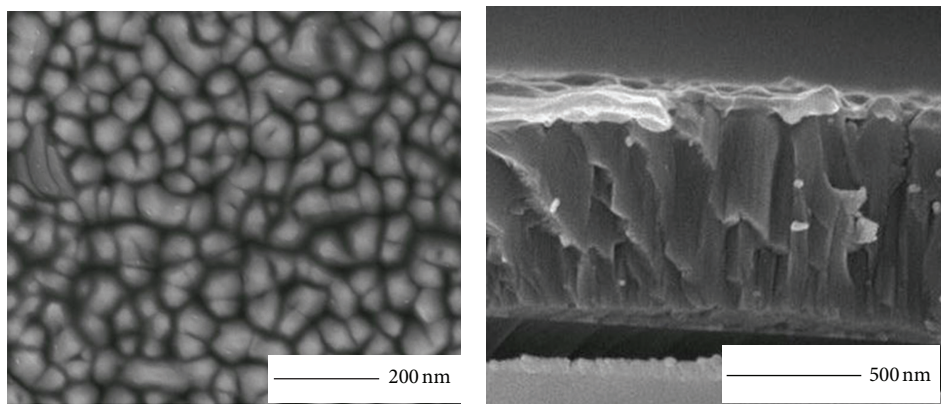

Figure 2: The SEM morphologies of the AlN film prepared at the laser energy density of 3.5 J/cm^2. (a) Surface view; (b) cross-section view.

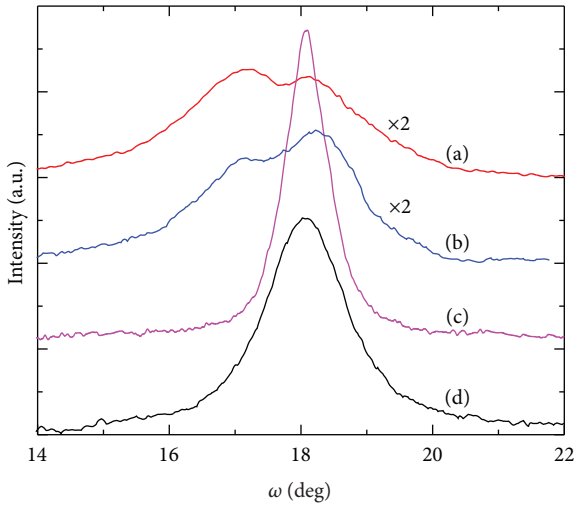

Figure 3: The (002) plane ω-scan rocking curves for AlN films prepared at laser energy density of (a) 1.3 J/cm^2, (b) 2.4 J/cm^2, (c) 3.5 J/cm^2, and (d) 4.8 J/cm^2.

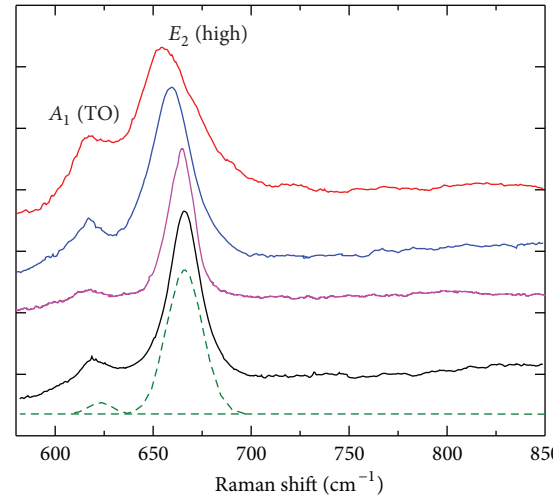

Figure 4: The Raman spectrum for AlN films prepared by PLD at laser energy density of (a) 1.3 J/cm^2, (b) 2.4 J/cm^2, (c) 3.5 J/cm^2, and (d) 4.8 J/cm^2.

optical (TO) components, thus creating A_1 (LO, TO) and E_1 (LO, TO) modes. The theoretical Raman scattering mode of the AlN film is summarized in Table 1.

The Raman spectra of the AlN films are shown in Figure 4. All samples exhibit two major Raman peaks around 660 cm^{-1} and 610 cm^{-1}, which correspond to E_2 (high) mode and A_1 (TO) mode. There are no obvious sapphire modes in the spectrum because the AlN films may be thick enough. In order to characterize the E_2 (high) peak and A_1 (TO) peak in detail, these two peaks were fitted by Lorentzian functions, whose fitting parameters are listed in Table 2. With the increase of the laser energy density, the A_1 (TO) peak becomes weak and the E_2 (high) peak becomes narrow. The spectrum of sample C has the smallest A_1 (TO) peak and the narrowest E_2 (high) peak.

3.3. The Correlation between the Raman Spectra and XRD Patterns. In order to find out the influence of the texture on the phone vibration in AlN films, the XRD and the Raman spectrum of each sample are compared as shown in Figure 5. For comparison, here the degree of (002) orientation of the films was defined as the ratio of the integrated area of (002) peak to the whole area in the XRD patterns. As for the Raman spectra, the FWHM of E_2 (high) peaks and the relative integrated areas of E_2 (high) mode were obtained from the fitting results. Some other samples prepared by 1–5 J/cm^2 laser were also involved. As shown in Figure 5, the correlation between the E_2 (high) mode and the (002) orientation degree is very clear. It is seen that the area of the E_2 (high) mode is larger for the films with higher (002) orientation. With the appearance of other orientation, the E_2 (high) area goes down while the A_1 (TO) mode is enhanced.

The close relationship between the Raman scattering modes and the film orientation can be explained using the Raman scattering rule as follows. Generally, the c-axis of the wurtzite unit cell is defined as z direction, and x and y are

Table 1: Raman scattering modes and their energies for unstrained AlN [3].

Mode	E_2 (low)	A_1 (TO)	E_2 (high)	E_1 (TO)	A_1 (LO)	E_1 (LO)
Energy (cm^{-1})	248.6 ± 0.2	611.0 ± 0.2	657.4 ± 0.2	670.8 ± 0.2	890.0 ± 0.2	912.0 ± 0.2

Table 2: The fitting parameters of A_1 (TO) and E_2 (high) peaks in the Raman spectrum of the AlN films prepared by PLD.

Sample	Laser energy density (J/cm^2)	A_1 (TO)			E_2 (high)		
		Center (cm^{-1})	FWHM (cm^{-1})	Area (%)	Center (cm^{-1})	FWHM (cm^{-1})	Area (%)
A	1.3	618.7 ± 0.4	15.5 ± 0.6	31.6 ± 2.1	657.2 ± 1.2	32.1 ± 1.5	65.4 ± 2.1
B	2.4	616.4 ± 0.3	11.7 ± 1.2	22.2 ± 1.1	659.6 ± 0.8	21.5 ± 0.5	71.1 ± 1.1
C	3.5	616.8 ± 0.5	19.7 ± 1.5	2.3 ± 0.2	663.3 ± 0.2	10.1 ± 0.3	97.7 ± 0.2
D	4.8	620.4 ± 0.4	10.6 ± 0.8	10.8 ± 1.8	665.1 ± 0.5	14.3 ± 0.7	89.2 ± 1.3

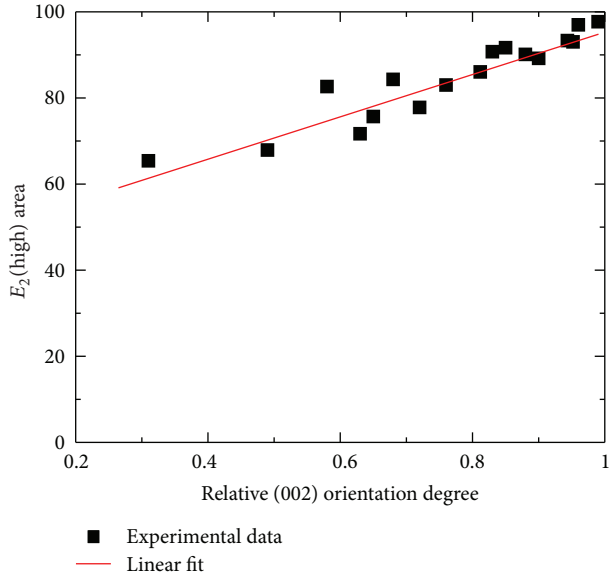

Figure 5: The relation between the relative integrated areas of the E_2 (high) scattering mode and the (002) orientation degree.

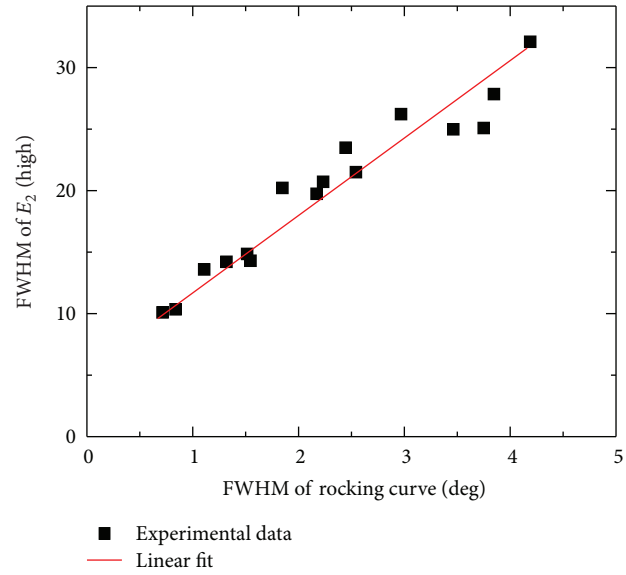

Figure 6: The FWHM of E_2 (high) peaks in Raman spectra as the function of the FWHM of the (002) peaks in X-ray rocking curves.

perpendicular to c axis. According to the Raman scattering rule of AlN [9], the E_2 (high) vibration mode is excited by an electric field perpendicular to z direction, while the A_1 (TO) mode is excited by an electric field parallel to z direction. In this experiment, the direction of propagation of Ar^+ laser is parallel to c-axis (z direction) and the backscattering geometry is equivalent to $z(xy)\bar{z}$ in the grains with the perfect (002) orientation. So the E_2 (high) mode is allowed for the high (002) orientated AlN films and thus the A_1 (TO) mode is forbidden. However, for the grains with multiple orientations, the electric field has the components parallel and perpendicular to c-axis, which excites both of the E_2 (high) and the A_1 (TO) modes. Consequently, the deterioration of (002) orientation and the appearance of other orientations in the films lead to the enhancement of the A_1 (TO) mode.

In addition, the broadening of the Raman peaks is the result of the phonon scattering caused by small grains, point defects, interfaces, and stress gradients [21]. In this experiment, we can reasonably assume that there is no strong stress gradients present in the films. The FWHM of the E_2 (high) peaks of the AlN films prepared by PLD varied from 10.1 to 32.1 cm^{-1}, which are intermediate between the 3 cm^{-1} reported by Kuball et al. [22] for the AlN bulk crystals and the 50 cm^{-1} reported by Perlin et al. [23] for highly defective crystals. In order to explain the broadening of Raman peaks, the FWHM of the E_2 (high) peaks as the function of the FWHM of XRD rocking curve is shown in Figure 6. The E_2 (high) peak is found to be broadened with the increase of the width of the X-ray rocking curve, suggesting that the broadening of the Raman peaks in the AlN films is associated with degeneration in crystal quality.

3.4. The Dependence of the Raman Spectra on the Residual Stress. The residual stress in the prepared film distorts the crystal unit cell, resulting in the variations on the energy of phonon vibration. Some authors [9, 21, 22, 24] have reported that the Raman peak spectrum can be used to monitor the stress in the films. Figure 7 shows the dependence of

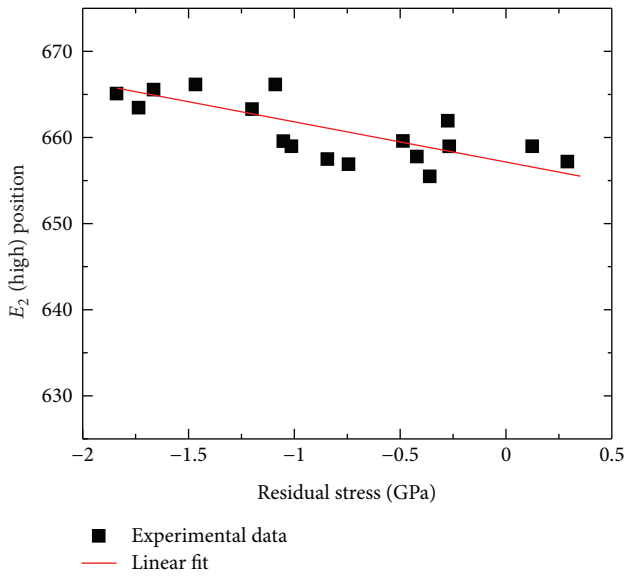

FIGURE 7: The dependence of E_2 (high) scattering mode energy on the residual stress of the AlN films prepared by PLD.

the measured E_2 (high) mode energy on the residual stress in the AlN films prepared by PLD. The residual stresses were calculated from the radius of the substrate curvature according to Stoney's equation. For the undoped AlN films under biaxial stress ($\sigma_\perp$) perpendicular to the growth c-axis, the shift in the phonon energy ($\Delta\omega$) can be written as

$$\Delta\omega = k\sigma_\perp, \quad (1)$$

where k is the Raman-stress factor. Tensile (compressive) stress corresponds to $\sigma_\perp > 0$ ($\sigma_\perp < 0$).

As shown in Figure 7, the E_2 (high) energy goes down nearly linearly with the decrease of the residual stress in the AlN films. Consequently, the Raman-stress factor can be obtained by combining the energy shift of E_2 (high) mode with the residual stress. The slope of the line provides the Raman-stress factor k of $-4.45\ \text{cm}^{-1}$/GPa in this experiment. This value is in accordance with the data reported in other papers [9, 21]. In addition, the zero-stress energy of $657.1\ \text{cm}^{-1}$ is also in good agreement with the value listed in Table 1.

4. Conclusions

We measured Raman spectra and XRD patterns of the AlN films prepared by PLD to study the influence of the crystal texture on the Raman scattering mode. The E_2 (high) mode and the A_1 (TO) mode were observed in Raman scattering. The orientation and the crystal quality of AlN films have a great impact on the scattering modes. The deterioration of (002) orientation and the appearance of other orientations lead to enhancement of A_1 (TO) mode in the films. The broadening of the Raman peaks can be associated with degeneration of the crystal quality. Additionally, by combining the energy shift of E_2 (high) mode with the measured residual stress, the Raman-stress factor of the AlN films prepared by PLD is found to be $-4.45\ \text{cm}^{-1}$/GPa for the E_2 (high) mode. These results indicate that Raman scattering is a feasible method to detect the crystal texture and residual stress of AlN films. In the further experiment, the luminous and electrical characteristics of the AlN films will be studied for their optical-electrical applications.

Acknowledgments

This work was supported by the National Science Foundation of China no. 61101027, Qingdao Science and Technology Program of Basic Research Projects (11-2-4-4-(6)-jch, 12-1-4-6-(8)-jch), Shandong Province Young and Middle-Aged Scientists Research Awards Fund (BS2012DX032), and SDUST Research fund (2011KYJQ101).

References

[1] G. Erkens, R. Cremer, T. Hamoudi et al., "Properties and performance of high aluminum containing (Ti,Al)N based supernitride coatings in innovative cutting applications," *Surface and Coatings Technology*, vol. 177-178, pp. 727–734, 2004.

[2] W. Xu, S. Choi, and J. Chae, "A contour-mode film bulk acoustic resonator of high quality factor in a liquid environment for biosensing applications," *Applied Physics Letters*, vol. 96, no. 5, pp. 053703–053705, 2010.

[3] Q. Wang, Y. P. Gong, J. F. Zhang, J. Bai, F. Ranalli, and T. Wang, "Stimulated emission at 340 nm from AlGaN multiple quantum well grown using high temperature AlN buffer technologies on sapphire," *Applied Physics Letters*, vol. 95, no. 16, Article ID 161904, 2009.

[4] C. Men, Z. Xu, Z. An et al., "Fabrication of SOI structure with AlN film as buried insulator by Ion-Cut process," *Applied Surface Science*, vol. 199, no. 1–4, pp. 287–292, 2002.

[5] D. Chen, D. Xu, J. Wang, B. Zhao, and Y. Zhang, "Dry etching of AlN films using the plasma generated by fluoride," *Vacuum*, vol. 83, no. 2, pp. 282–285, 2008.

[6] N. Sinha, G. E. Wabiszewski, R. Mahameed et al., "Piezoelectric aluminum nitride nanoelectromechanical actuators," *Applied Physics Letters*, vol. 95, no. 5, Article ID 053106, 2009.

[7] Y. Taniyasu, M. Kasu, and T. Makimoto, "An aluminium nitride light-emitting diode with a wavelength of 210 nanometres," *Nature*, vol. 441, no. 7091, pp. 325–328, 2006.

[8] T. Toyama, J. Ota, D. Adachi, Y. Niioka, D. H. Lee, and H. Okamoto, "Ultraviolet-light-emitting AlN:Gd thin-film electroluminescence device using an energy transfer from $Gd3^+$ ions to N_2 molecules," *Journal of Applied Physics*, vol. 105, no. 8, Article ID 084512, 2009.

[9] T. Prokofyeva, M. Seon, J. Vanbuskirk et al., "Vibrational properties of AIN grown on (111)-oriented silicon," *Physical Review B*, vol. 63, no. 12, pp. 1253131–1253137, 2001.

[10] A. M. Dabiran, A. M. Wowchak, A. Osinsky et al., "Very high channel conductivity in low-defect AlN/GaN high electron mobility transistor structures," *Applied Physics Letters*, vol. 93, no. 8, Article ID 082111, 2008.

[11] K. S. Zhuravlev, V. G. Mansurov, D. Y. Protasov, A. Y. Polyakov, N. B. Smirnov, and A. V. Govorkov, "Electrical properties and deep traps spectra of N-polar and Ga-polar AlGaN films grown by molecular beam epitaxy in a wide composition range,"

Journal of Applied Physics, vol. 105, no. 11, Article ID 113712, 2009.

[12] Y. Deng, Y. Kong, Y. Zheng et al., "Study on strain and piezoelectric polarization of AlN thin films grown on Si," *Journal of Vacuum Science and Technology A*, vol. 23, no. 4, pp. 628–630, 2005.

[13] Z. J. Reitmeier, S. Einfeldt, R. F. Davis, X. Zhang, X. Fang, and S. Mahajan, "Surface and defect microstructure of GaN and AlN layers grown on hydrogen-etched 6H-SiC(0001) substrates," *Acta Materialia*, vol. 58, no. 6, pp. 2165–2175, 2010.

[14] K. Sumitani, R. Ohtani, T. Yoshida, Y. Nakagawa, S. Mohri, and T. Yoshitake, "Influences of repetition rate of laser pulses on growth of crystalline AlN films on sapphire(0001) substrates by pulsed laser deposition," *Diamond and Related Materials*, vol. 19, no. 5-6, pp. 618–620, 2010.

[15] A. Szekeres, S. Bakalova, S. Grigorescu et al., "AlN:Cr thin films synthesized by pulsed laser deposition: studies by X-ray diffraction and spectroscopic ellipsometry," *Applied Surface Science*, vol. 255, no. 10, pp. 5271–5274, 2009.

[16] J. Ohta, H. Fujioka, H. Takahashi, and M. Oshima, "Growth of epitaxial AlN films on (Mn,Zn)Fe_2O_4 substrates by pulsed laser deposition," *Applied Surface Science*, vol. 197-198, pp. 486–489, 2002.

[17] S. H. Zhao, S. R. Dong, H. J. Zhang, W. W. Cheng, and X. X. Han, "Modeling of RF filter component based on film bulk acoustic resonator," *IEEE Transactions on Consumer Electronics*, vol. 55, no. 2, pp. 351–355, 2009.

[18] V. Brien and P. Pigeat, "Microstructures diagram of magnetron sputtered AlN deposits: amorphous and nanostructured films," *Journal of Crystal Growth*, vol. 299, no. 1, pp. 189–194, 2007.

[19] V. Y. Davydov, Y. E. Kitaev, I. N. Goncharuk et al., "Phonon dispersion and Raman scattering in hexagonal GaN and AIN," *Physical Review B*, vol. 58, no. 19, pp. 12899–12907, 1998.

[20] G. Shukla and A. Khare, "Dependence of N_2 pressure on the crystal structure and surface quality of AlN thin films deposited via pulsed laser deposition technique at room temperature," *Applied Surface Science*, vol. 255, no. 5, pp. 2057–2062, 2008.

[21] V. Lughi and D. R. Clarke, "Defect and stress characterization of AlN films by Raman spectroscopy," *Applied Physics Letters*, vol. 89, no. 24, Article ID 241911, 3 pages, 2006.

[22] M. Kuball, J. M. Hayes, A. D. Prins et al., "Raman scattering studies on single-crystalline bulk AIN under high pressures," *Applied Physics Letters*, vol. 78, no. 6, pp. 724–726, 2001.

[23] P. Perlin, A. Polian, and T. Suski, "Raman-scattering studies of aluminum nitride at high pressure," *Physical Review B*, vol. 47, no. 5, pp. 2874–2877, 1993.

[24] A. R. Goñi, H. Siegle, K. Syassen, C. Thomsen, and J. M. Wagner, "Effect of pressure on optical phonon modes and transverse effective charges in GaN and AlN," *Physical Review B*, vol. 64, no. 3, Article ID 035205, pp. 0352051–0352056, 2001.